

Synthesis and *in silico* investigation of Schiff base derivatives of 1*H*-indole-2,3-diones and their Co(II) and Ni(II) complexes as antimicrobial agents

Helen O. Echekwube¹, Pius O. Ukoha¹, Oguejiofo T. Ujam¹, Charles O. Nwuche^{2,*}, Jonnie N. Asegbeloyin¹ and Akachukwu Ibezim³

¹Department of Pure and Industrial Chemistry, University of Nigeria, Nsukka 410001, Enugu State Nigeria.

²Department of Microbiology, University of Nigeria, Nsukka 410001, Enugu State Nigeria. *Email: charles.nwuche@unn.edu.ng.

³Department of Pharmaceutical and Medicinal Chemistry, University of Nigeria, Nsukka 410001, Enugu State Nigeria.

Abstract. 3-[(2-aminophenyl)imino]-1,3-dihydro-2*H*-indol-2-one, (Lo), 1,3-phenylenediazanylylidene di (1,3-dihydro-2*H*-indol-2-one), (Lm) and 1,4-phenylenediazanylylidene di(1,3-dihydro-2*H*-indol-2-one) (Lp) were synthesized by the reaction of 1*H*-indole-2,3-dione with benzene-1,2-diamine, benzene-1,3-diamine and benzene-1,4-diamine respectively. The reaction of Lo, Lm and Lp with Co(II) and Ni(II) halides gave the corresponding coordination complexes which were characterized by elemental analysis, molar conductance, infrared, GC-MS and electronic spectral studies. Docking of the 1*H*-indole-2,3-diones toward the binding sites of penicillin binding protein and DNA gyrase showed they interacted favourably with the test antibacterial targets at ΔG s range of -2.51 to -5.48 kcal/mol. In accordance to literature report, coordination of cobalt and nickel to the ligands yielded metal complexes which exhibited improved interaction with the protein targets (at ΔG s range of -8.70 to -10.20 kcal/mol). *In vitro* antimicrobial studies against some microorganisms showed that some of the compounds were active against few Gram negative and Gram positive bacteria. The Lo, Lm and Lp had no activity against any of the test microorganisms but the Co(II) and Ni(II) complexes, showed antibacterial activity. The [Co(Lo)₂] and [Ni(Lo)₂] complexes generated the least antibacterial response. [Co(Lo)₂] was ineffective against *E. coli* 6 and *Staphylococcus sciuri subsp sciuri* while *Bacillus subtilis* was resistant to [Ni(Lo)₂] which moderately inhibited *E. coli* 14 (7 mm). Both compounds indicated zero activity against *Pseudomonas aeruginosa*. The complex that evoked the highest bactericidal activity were [CoLm]Cl₂ and [NiLp]Cl₂. The antibiogram activity of [CoLm]Cl₂ was found between 20 and 30 mm with *E. coli* 6 displaying greater sensitivity (30 mm) and *S. sciuri* the least (20 mm). The activity of [NiLp]Cl₂ complex indicate that the activity spectrum of the organisms occurred within 29 and 45 mm range; the least

Received
January 23, 2019

Accepted
April 24, 2019

Released
April 30, 2019



Full Text Article



ORCID

- 0000-0002-6490-3589
Helen O. Echekwube
- 0000-0003-3041-0919
Pius O. Ukoha
- 0000-0002-5628-209X
Oguejiofo T. Ujam
- 0000-0003-3914-1196
Charles O. Nwuche
- 0000-0002-5710-7613
Jonnie N. Asegbeloyin
- 0000-0003-1620-5716
Akachukwu Ibezim

sensitive were *E. coli* 14 (29 mm) and *B. subtilis* (29 mm) while the most sensitive was *S. sciuri subsp sciuri* (45 mm). The two compounds were further studied for minimum inhibitory concentration (MIC) and their binding modes towards the studied protein targets were analyzed. Result indicate that the MIC of 1.25 µg/mL was determined for the complex $[\text{NiLp}]\text{Cl}_2$ against *S. sciuri subsp sciuri* (12 mm) while in case of $[\text{CoLm}]\text{Cl}_2$, the MIC was 2.5µg/mL (13 mm) against the same organism. The binding modes predicted for $[\text{CoLm}]\text{Cl}_2$ and $[\text{NiLp}]\text{Cl}_2$ identified essential residues necessary for interaction with the studied proteins and which could be targeted during structural/activity optimization.

Keywords: 1*H*-Indole-2,3-dione; Anti-microbial activity; Physicochemical properties; Docking; Binding mode.

Introduction

Metal complexes play essential roles in biological, pharmaceutical and pharmacological processes. Some are essential for the normal functioning of living organisms (Housecroft and Sharpe, 2008) and many have been used as antibiotics against pathogenic microorganisms. However, in recent times, microorganisms have developed resistance against most of the existing antimicrobial agents, implying that infections caused by bacteria now constitute a serious burden to health care systems worldwide (Bollenbach, 2015). One way of controlling multidrug resistance of pathogenic microorganisms is by developing new bioactive compounds that are not based on existing synthetic antimicrobial agents.

1*H*-indole-2,3-dione, a well-known pharmacological privileged synthetic precursors for synthesis of bioactive compounds/agents has been known for about 150 years. Oxindole, a closely related polyfunctional heterocyclic derivative is an endogenous bioactive compound, widely distributed in mammalian tissues and body fluids (Medvedev et al., 1996; Silva et al., 2001). It also has analgesic and muscle relaxant effects (Chinnasamy et al., 2010). 1*H*-indole-2,3-dione derivative reportedly exhibit biological activities such as anti-bacterial (Varma and Nobles, 1975;

Pandeya and Sriram, 1998), anti-viral, anti-HIV(Pandeya et al., 1999; Pandeya et al., 2000a; Pandeya et al., 2000b), anti-protozoal (Imam and Varma, 1975; Varma and Khan, 1977), anti-allergic (Saranagapani and Reddy, 1977) and anti-inflammatory activities (Todeschini et al., 1998). The indole ring system affords a synthetic nucleus of interest in the search for new pharmaceutical agents (Bhrigu et al., 2010).

Literature search revealed very few anti-pathogen investigations involving Schiff bases of 1*H*-indole-2,3-dione and benzenediamines. 1*H*-Indole-2,3-dione derivatives have been described as potential drug candidates because Schiff bases of benzenediamine and their metal complexes have clinical and biological activities (Singh et al., 2010).

The fact that oxindole exists naturally in biological systems indicates that coordination complexes of 1*H*-indole-2,3-dione derivatives with bio-friendly metal ions can potentially have a good protein binding/docking ability against disease causing pathogens. Coordinated metal ions are known to accelerate drug actions and improve antimicrobial activities of bioactive ligands (Silva et al., 2001). However, in order to clearly understand the role of metal ions against pathogens, study of the structural and biological binding features of any metal complexes drug

candidate. This can help in better elucidation of the complexities of the bioprocess of drug actions. To the best of our knowledge such study has not been reported of 1H-indole-2,3-dione and benzendiamine derivatives.

In this report, we employed combine computational and experimental techniques to screen 1H-indole-2,3-dione Schiff bases derivatives of benzene-1,2-diamine, benzene-1,3-diamine and benzene-1,4-diaminebenzene and their Co(II) and Ni(II) coordination complexes for antibacterial action.

Material and methods

All the solvents methanol (May and Baker) and DMF (Kermel) are of analytical grade and were used as supplied. Ethanol, 1H-indole-2,3-dione, benzene-1,2-diamine, benzene-1,3-diamine and benzene-1,4-diamine and dimethylsulfoxide were supplied by Sigma-Aldrich, whereas cobalt(III) chloride hexahydrate ($\text{CoCl}_2 \cdot 6\text{H}_2\text{O}$), nickel(II)chloride hexahydrate, ($\text{NiCl}_2 \cdot 6\text{H}_2\text{O}$) camphor and paraffin were supplied by Wilkinson-Vickers Ltd. The ligands 3-[(2-aminophenyl)imino]-1,3-dihydro-2H-indol-2-one, Lo (Niume et al., 1982; Manan et al., 2012), 1,3-phenylenediazanylylidenedi(1,3-dihydro-2H-indol-2-one), Lm and 1,4-phenylenediazanylylidene di(1,3-dihydro-2H-indol-2-one) Lp (Wu and Gao, 2004; Singh, 2012) were synthesized according to literature procedures. $[\text{Co}(\text{Lo})_2]$, (1) was synthesized by modification of the literature procedure (Manan et al., 2012). Nutrient Agar (Lab M), and the controls, gentamicin, chloramphenicol and ampicillin were supplied by Lek Pharmaceutical and Chemical Company (Slovenia), and ciprofloxacin by May and Baker.

The ^{13}C and ^1H NMR data were obtained on a JEOL AV 400 spectrophotometer at 400 MHz in DMSO-d_6 and CDCl_3 with tetramethylsilane

(TMS) as internal standard. Infrared spectra were recorded on Shimadzu FTIR-8400S Fourier Transform infrared spectrophotometer in KBr disc. Electronic spectra were obtained on UVvis spectrophotometer 2500 PC series. The mass spectra were recorded on GCMS-QP 2010 Plus Shimadzu, Japan, at Narict, Zaria, Nigeria. The ^{13}C and ^1H NMR were obtained at University of Strathclyde, Glasgow. Elemental composition was determined using Perkin Elmer 2400 CHN Elemental Analyzer at Department of Pharmaceutical Sciences, University of Strathclyde, Glasgow. Melting points of the compounds were determined using a 4017 model of John-Fisher melting point apparatus. Molar conductivities of the complexes were measured in 10^{-3} M methanol solution using WTW LF90 conductivity meter made in Germany. All sterilization of materials for antimicrobial analysis were done in CV11/1000 autoclave machine with serial number A-4050. All incubations during antimicrobial analysis were done in a VT5042, EK/N2 Model of Heraeus incubator with serial number 0600341.

Preparation of metal complexes of 1H-indole-2,3-dione

Synthesis of 2-(aminophenyl)imino-1,3-dihydro-2H-indol-2-one-

Co(II), $[\text{Co}(\text{Lo})_2]$, (1). 2-(aminophenyl)imino-1,3-dihydro-2H-indol-2-one (Lo) (1 g, 4.2 mmol) dissolved in absolute ethanol (150 mL) was mixed with cobalt(II)chloride hexahydrate (0.5 g, 2.1 mmol) dissolved in absolute ethanol (20 mL). The resulting dark green mixture was refluxed at 50 °C in a water bath with constant stirring for 3 h. The solution changed to yellowish brown after 1 h 30 min. The solution was rotary evaporated to half the volume, and left in a refrigerator for 24 h. Lemon-yellow crystals formed were gravity filtered and recrystallized from absolute ethanol to yield yellow needle-like crystals (0.8 g, 71.4%).

Found: C, 64.9; H, 3.8; N, 16.7.

Calc. C, 63.0; H, 3.8; N, 15.8.

Melting Point: 248 °C

IR_{vmax}: 3397, 1574, 1662 cm⁻¹

¹H NMR (CDCl₃, 400 MHz): δ 12.48 ppm (N-H), 6.45 (N-H), 6.8 - 7.8 ppm (Ar proton)

¹³C NMR (CDCl₃, 400 MHz): δ 155.30 ppm (C=N), 132.01 ppm (C-NH₂), 118.06-131.29 ppm (Ar-C-H)

Synthesis of 2-(aminophenyl) imino-1,3-dihydro-2H-indol-2-one-

Ni(II), [Ni(Lo)₂], (2). 2-(aminophenyl) imino-1,3-dihydro-2H-indol-2-one (Lo) (1 g, 4.2 mmol) dissolved in absolute ethanol (150 mL) in 500 mL round bottomed flask was added nickel(II)chloride hexahydrate (0.5 g, 2.1 mmol) dissolved in ethanol (10 mL). The resulting yellowish-orange mixture was refluxed at 50 °C in a water bath with constant stirring for 3 h. The solution on cooling yielded yellow precipitates that were gravity filtered and recrystallized from absolute ethanol (0.72 g, 64%).

Found. C, 69.3; H, 5.1; N, 15.1.

Calc. C, 63.1; H, 4.2; N, 15.8

Melting Point: 244 °C

IR_{vmax}: 3408, 1591, 1661 cm⁻¹

¹H NMR (CDCl₃, 400 MHz): 7.14-7.58 ppm (Ar-H), 7.78-7.8 (Ar-H), 6.45 ppm (N-H)

12.47 ppm, (N-H Indole ring)

¹³C NMR (CDCl₃, 400 MHz): 156.50 ppm (C=O), 155.29 (C=N), 123.81-144.58 ppm (Ar-C)

Synthesis of 1,3-phenylenediazanylylidene di(1,3-dihydro-2H-indol-2-one)Co(II) dichloride [CoLm]Cl₂, (3).

1,3-Phenylenediazanylylidene di(1,3-dihydro-2H-indol-2-one) (1 g, 2.73 mmol) dissolved in hot absolute ethanol (200 mL) in 250 mL round bottomed flask was added cobalt(II) chloride hexahydrate (0.32 g, 1.3 mmol) dissolved in absolute ethanol (10 mL). The resulting brown solution was stirred and refluxed for 3 h

at 50 °C. The solution was concentrated to half the volume and kept at room temperature for two days to crystallize. The brown precipitates of the product was gravity filtered and recrystallized from ethanol and air dried (0.67 g, 16.5%)

Found C, 58.3; H, 4.8; N, 12.7.

Calc. C, 53.3; H, 2.8; N, 15.3

Melting Point: 316 °C

IR_{vmax}: 3374, 1725, 1622 cm⁻¹

¹H NMR(CDCl₃, 400 MHz): 6.88-6.92 ppm (Ar-H indole), 10.89 ppm (N-H), 6.73-6.79 (Ar-H)

¹³C NMR(CDCl₃, 400 MHz): 184.96 ppm (C = O), 159.91 ppm (C = N), 112.81-151.28 ppm (Ar-C).

Synthesis of 1,3-phenylenediazanylylidene di(1,3-dihydro-2H-indol-2-one)Ni(II) dichloride [NiLm]Cl₂, (4).

Nickel(II)chloride hexahydrate (0.32 g, 1.36 mmol) dissolved in absolute ethanol (10 mL) was mixed with 1,3-phenylenediazanylylidenedi(1,3-dihydro-2H-indol-2-one) (1 g, 2.73 mmol) dissolved in ethanol (200 mL) in a 250 mL round bottomed flask. The light brown solution was refluxed for 3 h at 50 °C. The solution turned dark brown and was evaporated to half the volume and allowed to cool to room temperature to form precipitates. Dark brown precipitate of the product was filtered and recrystallized from methanol to give, 0.7 g, 17.2%.

Found C, 50; H, 4.1; N, 9.0. Calc. C, 53.3; H, 2.8; N, 15.3

Melting Point: 296 °C

IR_{vmax}: 3041, 1700, 1620 cm⁻¹

¹H NMR (CDCl₃, 400 MHz): 6.78-6.90 ppm (Ar-H indole), 10.80 ppm (NH indole), 6.70-6.70 - 6.70 - 6.89 ppm (Ar-H)

¹³C NMR (CDCl₃, 400 MHz): 184.86 ppm (C = O), 159.96 ppm (C = N), 112.80-15128 (Ar-C)

Synthesis of 1,4-phenylenediazanylylidenedi(1,3-dihydro-2H-indol-2-one)dichloro cobalt (II), [CoLpCl₂], (5). 1,4-Phenylenediazanylylidene di(1,3-dihydro-2H-indol-2-one) (3 g, 8.19 mmol) dissolved in 10 mL dimethylformamide (DMF) was mixed with cobalt(II)chloride hexahydrate dissolved in 5 mL DMF in a 250 mL round bottomed flask. The stirred mixture was refluxed for 3 h at 50 °C. The dark red solution gradually changed to dark brown forming dark brown precipitates. The dark brown precipitate was gravity filtered and washed with diethyl ether (4 x 10 mL) to yield 2.1 g, 51.7 % of the complex.

Found C, 56.9; H, 2.84; N, 10.6.
Calc. C, 53.3; H, 3.51; N, 11.3
Melting Point: 300 °C

IR_{vmax}: 3445, 1734.06, 1614.47 cm⁻¹

¹H NMR (CDCl₃, 400 MHz): 7.49-7.91 ppm (Ar-H), 11.04 ppm (N-H indole ring)

¹³C NMR (CDCl₃, 400 MHz): 164.09-164.15 ppm (C=O) 155.23-159.24 ppm (C=N), 111.33-119.68 ppm (Ar-C-H).

Synthesis of 1,4-phenylenediazanylylidenedi(1,3-dihydro-2H-indol-2-one)nickel(II) dichloride, [NiLp]Cl₂, (6). 1,4-Phenylenediazanylylidene di(1,3-dihydro-2H-indol-2-one) (3 g, 8.19 mmol) dissolved in DMF (120 mL) in a 250 mL flask was mixed with nickel(II) chloride hexahydrate dissolved in DMF (5 mL). The solution (pale red) was stirred for 20 min at room temperature yielded brown precipitates which were filtered and washed with diethyl ether (3 x 10 mL) and ethanol (3 x 10 mL). The product was recrystallized from methanol (yield = 2.2 g, 54.2%).

Found C, 51.2; H, 3.5; N, 10.9.
Calc. C, 53.3; H, 2.9; N, 11.3
Melting Point: 274 °C

IR_{vmax}: cm⁻¹ 3425, 1716.70, 1615.44

¹H NMR (CDCl₃, 400 MHz): 7.47-7.82 ppm (Ar-C-H), 11.14 ppm (N-H)

¹³C NMR (CDCl₃, 400 MHz): 164.16-164.36 ppm (C=O), 155.32-160.1 ppm (C=N), 112.14-119.15 ppm (Ar-C-H)

Simulation studies

Three dimensional chemical structures of 1H-Indole-2,3-diones and their metal complexes were generated using the graphical user interface of molecular operating environment (MOE) software running on a Linux workstation with a 3.5 GHz Intel Core 2 Duo processor and energy minimized using the MMFF94 force field available in MOE minimization module until a 0.01 kcal/mol energy was reached (CCG, 2010; Halgren, 1996). The molecular weight (MW), lipophilicity (log P), hydrogen bond acceptor/donor (HBA/HBD) and number of rotatable bonds (NRB), of the compounds were computed using the QuSAR module implemented in MOE.

The x-ray crystal structures of the protein targets (penicillin binding protein (PBP) and DNA gyrase with their cocrystallized inhibitors) employed in this study were retrieved from protein data bank (PDB codes: 1CEF and 1KZN respectively) according to Berman et al., (2000). The complex dimers were treated using MOE as described in our earlier works (Ibezim et al., 2016; Ibezim et al., 2017a; Ibezim et al., 2017b).

Docking calculations of the compounds were carried out using AutoDock4.2.0 (Morris et al., 1998). The dock protocol employed was validated by several trials to obtain one that respects the root mean square deviation method as shown in results and discussion section.

Biological screening

Microorganisms and culture conditions. Four bacterial strains were used in the present study. The organisms

were obtained from the stock collections of the Veterinary Teaching Hospital, Faculty of Veterinary Medicine, University of Nigeria, Nsukka. The Gram negative organisms were *Escherichia coli* 14 ATCC 25922, *Escherichia coli* 6 ATCC 11105, and *Pseudomonas aeruginosa* ATCC 27853. The Gram positives were *Bacillus subtilis* (isolated and maintained in our laboratory) and *Staphylococcus sciuri sub sp sciuri* ATCC 29062. One loopful of each bacteria strain was reactivated by transferring into nutrient both (NB) (Lab M) and incubated at 37 °C for 24 h except for *B. subtilis* which was kept at 30 °C.

Antimicrobial susceptibility testing. The agar well diffusion method of Tag and Mcgiven (1971) was used in determining the antimicrobial properties of the synthesized compounds while the minimum inhibitory concentration (MIC) was evaluated by the broth dilution technique approved by the National Committee for Clinical Laboratory Standards (NCCLS, 1993).

Agar well diffusion. Fresh stock solutions of the synthesized complexes and their ligands were dissolved in 30% dimethylsulfoxide (DMSO; BDH, Milan, Italy) to a final concentration of 20 µg/mL. The inoculum suspension of each test bacterium were prepared from overnight broth cultures and the turbidity equivalent adjusted to 0.5 McFarland standard gave a concentration of 1.5×10^8 cfu/mL. In order to determine the antimicrobial activity of each compound, 100 µl of each bacterial suspension was uniformly smeared on the surface of Petri dishes into which sterile 20 mL each of Mueller-Hinton Agar (MHA) had been previously added, cooled and pre-dried. Excess inoculum was removed by a sterile syringe before allowing drying for 20 min at room temperature. Wells (6mm diameter; 24mm apart) were aseptically made on the surface of each agar plate using a flamed cork borer. Subsequently,

50 µL of each compound dissolved in DMSO was introduced into the wells of the already seeded MHA plates. Other wells contained ampicillin, ciprofloxacin and gentamicin at 20 µg/mL as positive controls while DMSO was included as negative control. Plates inoculated with each test bacterium were incubated at 37 °C for 24 h with the exception of *B. subtilis* which was maintained at 30 °C for 24 h. After incubation, the diameters of the inhibition zones formed on the MHA plates were determined (in millimeters) against a metre rule using a pair of dividers. Zones of inhibition of complexes and ligands were considered after subtracting the inhibition zone of DMSO. The data obtained were compared to the inhibition zone diameters (IZD) of the reference antibiotics used as positive control. All the experiments were performed in triplicates and reported data are presented as average of obtained results.

Minimum inhibitory concentration (MIC)

Compounds with promising antimicrobial properties were selected for minimum inhibitory concentration (MIC) studies. The MIC was determined using serially diluted stock solutions of the complexes and their ligands in DMSO. The agar-well diffusion technique was repeated. The test bacteria were inoculated into nutrient broth. Cultures were grown at 30 °C-37 °C for 18 h - 24 h to density of 10^6 cfu/mL. The inoculum was again adjusted according to 0.5 McFarland standards and used to seed freshly prepared MHA plates. Initially, 100 µL of Mueller Hinton Broth (MHB) was placed in each well. After, the compounds were dissolved in DMSO (2 mg/mL) and transferred into the first well. A 2-fold dilution of the compounds was made to achieve a decreasing concentration of 10 to 1.25 µg/mL for MIC determination. The wells were filled with 50 µL of each dilution, allowed to stabilize before incubating the plates for 24 h at 30 °C - 37 °C. During this period,

the test solution diffused into the agar and the growth of the inoculated microorganisms was affected. The inhibition zones of the various dilutions were noted. The lowest concentration of each study compound that resulted in the complete inhibition of the test microorganisms was reported as the MIC ($\mu\text{g/mL}$). Similar procedure was performed with the positive controls - ampicillin, ciprofloxacin and gentamicin and their MIC recorded for comparison. Tests were performed in triplicate and results expressed as means.

Results and discussion

Synthesis and characterization of 1H-indole-2,3-diones and their complexes

Reaction ratios of the ligands and metal salts were predetermined by the Job's continuous variation method (supplementary data). The reaction of $\text{CoCl}_2 \cdot 6\text{H}_2\text{O}$, 1a, with excess 2-(aminophenyl) imino-1,3-dihydro-2H-indol-2-one, Lo, initially gave a yellowish brown solution which upon refluxing turned yellowish brown from which lemon-yellow crystals of the product were recovered by concentration and precipitation. Analysis of the solid by GSMS showed a dominant ion at $m/z = 533.3$ which was assigned to the complexes species $[\text{Co}(\text{Lo})_2]$, 1 (calculated $m/z = 533.45$) due to good agreement between the two values. The reaction of Lo with $\text{NiCl}_2 \cdot 6\text{H}_2\text{O}$, 1b, gave initial yellow-brown solution from which the corresponding pale yellow precipitate of the nickel complex

$[\text{Ni}(\text{Lo})_2]$, 2 with GSMS prominent ion peak at $m/z = 540.5$. No reaction was observed on addition of aqueous AgNO_3 to solutions of 1 and 2. The reactions of 1,3-phenylenediazanylylidene di(1,3-dihydro-2H-indol-2-one) (Lm) with, with 1a and 1b gave dark brown complexes, $[\text{CoLmCl}_2]$, 3 and $[\text{NiLmCl}_2]$, 4, with $m/z = 497$ and $m/z = 495$ respectively. White precipitate was formed upon addition of drops of AgNO_3 solution to the solutions of the recrystallized 3 and 4. The reactions of 1,4-phenylenediazanylylidene di(1,3-dihydro-2H-indol-2-one) (Lp) with 1a and 1b gave the corresponding dark-brown precipitates of $[\text{CoLpCl}_2]$, 5 and $[\text{NiLpCl}_2]$, 6, which gave $m/z = 500$ and $m/z = 493.83$, respectively.

Conductivity

The electrolytic conductance of the complexes 1 and 2 in methanol are $14.88 \mu\text{Smol}^{-1}$ and $15.79 \mu\text{Smol}^{-1}$, respectively. The complexes have low electrolytic conductance compare to KCl, $114.38 \mu\text{Smol}^{-1}$. This indicates non-electrolytic nature of 1 and 2 and not appreciable dissociation in solution. In contrast 3 had an electrolytic conductance of $143.28 \mu\text{Smol}^{-1}$ which is higher than the value for the control (KCl). This indicates a 1:2 electrolyte (Singh et al., 2010; Kriza et al., 2011) implying non-bonding of chloride ion to the inner sphere of the Co(II) center and ionic nature of the complex (Mohamed et al., 2006). The molar conductance of 4, 5, 6 and KCl (Table 1) indicated appreciable ionization in solution and electrolytic nature.

Table 1. Molar conductivity of the complexes.

Complex	1	2	3	4	5	6	KCl
Molar Conductance (μSmol^{-1})	14.88	15.79	143.28	72.21	40.88	83.72	114.3

Infrared spectral properties

Infrared spectral data of Lo, Lm and Lp and [Co(Lo)₂] 1; [Ni(Lo)₂] 2, [CoLm]Cl₂ 3, [CoLm]Cl₂ 4, [CoLpCl₂] 5 and [NiLp]Cl₂ 6 are as shown in Table 2. Confirmatory IR characterization was performed of Lo before reacting with the metal salts. This was done to reassess contradictory reports in literature (Cerchiaro et al., 2006; Singh et al., 2010; Manan et al., 2012) that the two amino groups of benzene-1,2-diamine are involved in condensation with the two keto groups of 1*H*-indole-2,3-dione to give a cyclo compound. The IR spectrum of pure 1*H*-indole-2,3-dione shows two strong bands at 1740 cm⁻¹ and 1620 cm⁻¹ corresponding to the carbonyl stretching vibrations (Silva, 2001). The spectrum of benzene-1,2-diamine shows two medium

intensity bands at 3250 cm⁻¹ and 3280 cm⁻¹ due to $\nu(\text{NH}_2)$ (Singh, 2010). In the spectrum of Lo only one of the carbonyl stretching vibrations appeared at 1659 cm⁻¹ (Mashaly, et al., 2004; Singh, 2010). This evidently indicated that one of the carbonyl (C=O) groups of 1*H*-indole-2,3-dione condensed with one of the amino groups of benzene-1,2-diamine to form Lo. In addition, the formation of the Schiff base was indicated by the appearance of a strong band at 1591 cm⁻¹ attributable C=N stretching vibration (Raman et al., 2007; Singh et al., 2010).

The IR data of the ligands Lo, Lm and Lp and the metal complexes (Table 2) revealed the functional groups of ligands that coordinated to the central metal ions.

Table 2. IR spectral bands of Lo, Lm Lp and their Co(II) and Ni(II) complexes.

Lo	[Co(Lo) ₂]	[Ni(Lo) ₂]	Lm	[CoLm]Cl ₂	[NiLm]Cl ₂	Lp	[CoLpCl ₂]	[NiLp]Cl ₂	Assignments
3750 (w) 3640 (w)	-	-							NH ₂ , primary aromatic amine
3402 (m) 3250 (w)	3397 (s)	3408.33 (s)	3374 (b)	3374 (b)	3405 (b)	3449 (b) 3175 (s)	3446 (b) 3311 (b)	3426 (b) 3207 (s)	NH of indole ring
3085 2990(m)	3108 (m) 3000 (s)	3108.39 (m)						3095 (s) 2366 (s)	ν (C-H) phenyl
		3007.12 (m)	2366 (m)	2373	2362				ν (C-H) phenyl
2847 (m)	2851 (s)	2849.92 (m)							ν (C-H)
1660(s)	1662 (s)	1660.77 (m)	1721 (s)	1721	1700	1737 (s)	1734 (s)	1717 (s)	ν (C=O)
1591 (m)	1575 (s)	1591.33 (w)	162 (s)	16229 (s)	1620 (s)	1610 (s)	1615 (s)	1615 (s)	ν (C=N)
1429(w)	1438 (m)	1466.91 (w)	1476	1475	1477	1398 (m)	1403 (s)		ν (C-C) in plane vibration
1336 (w)	1329 (w) 1266 (w)	1329.96 (w)	1399 1333 (m)	13999 (s) 1331 (m) 1227 (w)	1388.79	1335 (s)	1332 (m) 1285 (w)	1374 (s) 1282 (w)	C-N stretching vibration.
1219(w)	1215 (w)	1217.12 (w)							N-H in plane bending.
1149 (w)	1168 (w)	1130 (w)							N-H in-plane bending.
1010 (w)		1003.02 (w)	1110 (w) 1208	1006 (w)	1100 (w)	1209 (s) 1150 (w)	1204 (w) 1150 (w)	1213 (w) 1159 (w)	C-H (phenyl) in-plane bend
901 (w)	896 (w)	897.89 (w)	852 (w)	850		994 (w)	948		N-H out-of-plane wagging
752 (s)	751 (s)	749.37 (s)	752 (m)	752 (m)	751 (w) 657 (w)	819 (m) 744 (s)	843 (m) 760 (w)	850 748 (m)	C-H out-of-plane bend (phenyl ring)
590 (w)	595 (w)	600.85 (w)	662 (w)					638 (m)	Out- of- plane ring bending.
483(w)	483 (w)	483.18 (w)	501						Out- of- plane ring bending
-	425 (w)			584 (w)	425 (w)		450		ν (M-N)
-	503	511.15		632 (w)	499 (w)		550	500	ν (M-O)

s=strong, m = medium, w = weak, b = broad [intensities].

Comparison of the IR spectrum of 1 with that of Lo as regards the $\nu(\text{NH}_2)$ bands revealed the conspicuous

disappearance of the doublet at 3750 cm⁻¹ and 3640 cm⁻¹ from the spectrum of the complex. This was presumably due to the

involvement of the primary amino group in coordination to the Co(II) ion. Another significant change in absorption is that of $\nu(\text{C}=\text{O})$ which was centred at 1660 cm^{-1} in the ligand shifted to 1662 cm^{-1} with increased intensity in the Co(II) complex. This is also indicative of possible weak coordination to the metal through the carbonyl group (Abdul-Manan, et al., 2017). This is confirmed by the appearance of a non-ligand band at 503 cm^{-1} in the cobalt complex spectrum assignable as $\nu(\text{Co}-\text{O})$ (Reddy et al., 2008). This observation is contrary to literature report (Manan et al., 2012) on this complex in which the indole keto group was not used in bonding with the Co(II) ion. The C=N stretching vibration centered at 1591 cm^{-1} in the ligand also shifted negatively to 1575 cm^{-1} on coordination with the metal, strongly indicating the involvement of the azomethine nitrogen in coordination (Hassan, 1991; Singh et al., 2010; Manan, et al., 2012). This shift to lower wavenumber may be explained on the basis of shift of electron density of azomethine nitrogen towards metal ion (Singh et al., 2010) leading to lowering of bond order (Manan et al., 2012). The involvement of azomethine nitrogen is further confirmed by the appearance of a new weak band centered at about 425 cm^{-1} in the complex which is absent in the ligand's spectrum. This band is attributable to $\nu(\text{Co}-\text{N})$ stretching vibration (Abdul-Manan et al., 2017; Reddy et al., 2008). The IR spectrum of the ligand and its Co(II) complex generally imply that Lo is tridentate coordinating to the Co^{2+} through C=O, NH_2 and C=N groups and this is in accordance with the proposed structure for the complex (Figure 1).

The Ni(II) complex, 2, IR absorption bands also revealed the absence of the $\nu(\text{NH}_2)$ doublet in the Ni(II) complex spectrum but which appeared at about 3750 cm^{-1} and 3640 cm^{-1} in the free ligand spectrum. The disappearance of these peaks on coordination of Lo to Ni(II) ion indicates

coordination occurred (Ukoha et al., 2011) via the nitrogen of the primary amino group. There was an upward shift in the stretching vibration of C=O group from 1660 cm^{-1} in the ligand to 1661 cm^{-1} in the Ni(II) complex with low intensity. This also indicates the possible weak participation of carbonyl oxygen in coordinating to Ni(II) ion (Hassani et al., 2011). The appearance of non-ligand band at 511 cm^{-1} in the spectrum of 2 which assignable to $\nu(\text{M}-\text{O})$ (Reddy et al., 2008; Abdul-Manan et al., 2017). The $\nu(\text{C}=\text{N})$ at 1591 cm^{-1} in the ligand remained unchanged in IR of 2 indicating that the azomethine nitrogen did not coordinate to Ni(II) ion (Hassani et al., 2011). The IR spectra of Lo and the Ni(II) complex suggests that Lo acted like a bidentate ligand in coordinating to Ni(II) ion through C=O and NH_2 groups.

The spectrum of the complex $[\text{CoLm}]\text{Cl}_2$ 3 had the intensities of ligand bands slightly changed which suggest ligation of the ligand to the Co(II) ion since shifts, weakening/change in intensities or absence of peaks of ligands on coordination to metal has been interpreted in terms of coordination through such functional groups (Mohamed et al., 2006; Ukoha et al., 2011). The $\nu(\text{N}-\text{H})$ of the indole moiety of the ligand at 3374 cm^{-1} remained unchanged both in position and intensity upon complexation with Co(II) ion indicating the non-involvement in coordination. The strong absorption band at 1721 cm^{-1} assigned to $\nu(\text{C}=\text{O})$ in the ligand remained as in position in the Co(II) complex, however the intensity of this band decreased in the complex presumably due to weak ligation (Mohamed et al., 2006; Ukoha et al., 2011). The azomethine $\nu(\text{C}=\text{N})$ in the Co(II) complex appeared at 1622 cm^{-1} just as in the ligand. However there was change in intensity due to ligation (Breitmaier and Voelter, 1987) to the Co(II) ion. The presence of the new weak bands at 632 cm^{-1} and also at 584 cm^{-1} in the metal complex spectrum which are absent in the ligand's spectrum indicated

coordination of ligand to the Co(II). These bands were assigned to $\nu(\text{M-O})$ stretching vibration and $\nu(\text{M-N})$ (Ukoha et al., 2011; Nagajothi et al., 2012) respectively. The IR spectra of the ligand and the Co(II) complex show that Lm is tetradentate but weakly coordinated through azomethine nitrogen and C=O.

The IR spectrum of $[\text{NiLm}]\text{Cl}_2$ 4 revealed the C=O stretching vibrations at 1721 cm^{-1} in the ligand almost disappeared from the spectrum of the metal complex. This indicate strong coordination to Ni(II) ion via the oxygen atom of C=O group. This observation is further strengthened by the appearance of a non-ligand band at 491 cm^{-1} in the spectrum of 4 assigned as $\nu(\text{M-O})$. The same conclusion has been drawn concerning Ni(II) complexes of 1*H*-indole-2,3-dione derivatives in the literature (Kriza et al., 2011; Nagajothi et al., 2012; Abdul-Manan et al., 2017). The absorption band at 1622 cm^{-1} assigned as C=N stretching vibration (Singh et al., 2010) in the ligand shifted to 1620 cm^{-1} with a decrease in intensity in the spectrum of 4. This is an indication of the ligand's coordination to Ni(II) ion through the azomethine nitrogen.

A new band at about 425 cm^{-1} was observed in the spectrum of 4 which is attributable to $\nu(\text{M-N})$ (Mashaly et al., 2004; Singh et al., 2010; Nagajothi et al., 2012). The N-H stretching vibration at 3374 cm^{-1} in the ligand, changed to 3401 cm^{-1} in 4 suggesting possible coordination to Ni(II) ion through the indole amino nitrogen atom. Also the N-H out-of-plane wagging vibration at 852 cm^{-1} in the free ligand was not observed in the spectrum of 4. This involvement of indole amino group in coordination to Ni(II) ion is contrary to literature reports (Reddy et al., 2008; A-Hassani et al., 2011; Kriza et al., 2011) concerning most related Ni(II) complexes of indole-2,3-dione Schiff bases. Comparison of the Lp IR bands with those of the 4 shows that the ligand is hexadentate coordinating to the Ni(II) ion via the two carbonyl

oxygen, two azomethine nitrogen and the two indole amino nitrogen atoms.

Comparison of the IR data of the ligand Lp with that of the 5 revealed that the absorption band of $>\text{C}=\text{O}$ group shifted from 1737 cm^{-1} to 1734 cm^{-1} , indicating possible involvement of the carbonyl oxygen in coordination to Co(II) ion. An upward shift of the $\nu(\text{C}=\text{N})$ from 1610 cm^{-1} in the free ligand to 1615 cm^{-1} in 5 and the appearance of new weak bands in the spectrum of 5 at about 525 cm^{-1} and 450 cm^{-1} attributed to M-O and M-N stretching vibrations (Reddy et al., 2008; Singh et al., 2010; Agbo and Ukoha, 2010) respectively suggested the coordination through the azomethine nitrogen atom. The IR data of Lp and its Co(II) complex generally imply that Lp coordinated as a tetradentate ligand through $>\text{C}=\text{O}$ and $>\text{C}=\text{N}$ groups.

The spectrum of $[\text{NiLp}]\text{Cl}_2$ 6 indicated a shift in the ligand's $>\text{C}=\text{O}$ stretching vibrations to lower wave number, from 1737 cm^{-1} (ligand) to 1716.70 cm^{-1} (complex), indicating bonding of $>\text{C}=\text{O}$ oxygen to Ni(II) ion. This is further confirmed by the appearance of non-ligand band in the spectrum of 6 at about 500 cm^{-1} assignable as $\nu(\text{M-O})$ (Reddy et al., 2008). The strong absorption band at 1615 cm^{-1} due to $\nu(\text{C}=\text{N})$ in 6 shifted from the Lp $\nu(\text{C}=\text{N})$ at 1609.65 cm^{-1} . This upward shift to higher wavenumber in the complex indicates ligation through the azomethine nitrogen. This disagrees with what has been documented in the literature (A-Hassani et al., 2011) for Ni(II) complex of Schiff base derived from condensation of 1*H*-indole-2,3-dione with benzene-1,4-diamine, in which the azomethine nitrogen did not coordinate to Ni(II) ion. The broad band at 3425 cm^{-1} assigned as $\nu(\text{NH})$ in the complex changed from Lp band at 3449 cm^{-1} indicating the involvement of the indole amino nitrogen in coordination. The IR spectral data of Lp and 6 suggest a hexadentate ligand coordinated via C=N, indole amino group and C=O group.

UV-vis Electronic Spectral Properties

The electronic spectral data of the ligands and complexes are presented

in Table 3. The electronic spectrum of Lo revealed two absorption bands at 440.4 cm⁻¹ and 353.4 cm⁻¹.

Table 3. UV-visible electronic spectral data of the ligands and their Co(II) and Ni(II) complexes.

Compound	nm (cm ⁻¹)	nm (cm ⁻¹)	nm(cm ⁻¹)	nm(cm ⁻¹)	nm (cm ⁻¹)	nm (cm ⁻¹)	nm (cm ⁻¹)
Lo	440.40br (22706.63)				353.40(s) (28296.55)		
[Co(Lo) ₂]	423.20w (23629.49)	421w (23741.69)	369.80w (27041.64)	359.60s (27808.68)	350.40 (28538.81)		
[Ni(Lo) ₂]					354.60s (28200.80)	≈342 (29239.80)	
Lm		414 br (24154.59)	297sh (33670.03)	276.50sh (36166.37)	268.50sh (37243.95)	257sh (38910.51)	
[Co(Lm)Cl ₂]	485.50 br (20597.32)	434 br (23041.47)	292 sh (34246.57)	283.50sh (35273.37)	267sh (37453.18)	259.50sh (38535.65)	
[Ni(Lm)Cl ₂]		429 br (23310.02)	292 sh (34246.58)	284.50sh (35149.38)	275sh (36363.63)	255sh (39215.69)	
Lp				611.60vw (16350.56)	441.60 br (22644.93)	364.40w (27442.37)	359w (27855.15)
[Co(Lp)Cl ₂]		627.40vw (15938.79)	413w (24213.08)	621.20vw (16097.88)	354.60w (28200.79)	364.60w (27427.32)	358.20w (27917.36)
[Ni(Lp)Cl ₂]	760.50w (13149.24)	741.50w (13486.18)	656w (15243.90)	625.50W (15987.21)	436w (22935.78)		

Intensities: Vw - very weak; br - broad, sh - shoulder; s - strong; Vs - very strong.

These bands are attributed to intra ligand $\pi^* \leftarrow n$ and $\pi^* \leftarrow \pi$ transitions respectively (Agbo and Ukoha, 2010; Ukoha et al., 2011). These transitions are due to benzene ring, the electron pair of N atom of azomethine/amino groups and the excitation of the lone pair of electrons on the oxygen atom of the .C=O group (Akpanisi, 2004). These transitions are all present in the Ni(II) and Co(II) complexes of Lo.

The spectrum of 1 showed the electronic bands of the ligand and additional bands at 23629.49 cm⁻¹, 23741.69 cm⁻¹, 27041.64 cm⁻¹, 27808.68 cm⁻¹ and 28538.81 cm⁻¹. The bands at 23629.49 cm⁻¹ and 28538.81 cm⁻¹ were attributed to intra-ligand $\pi^* \leftarrow \pi$ and $\pi^* \leftarrow n$ transition. Comparing these bands with those of the free ligands revealed shift to lower wavelengths which indicate some degree of non-bonding of the electrons on the hetero-atoms N and O due to ligation of the atoms to Co²⁺ during complex formation. The new absorption band at 23741.69 cm⁻¹ is

most likely due to *d-d* transition (⁴T_{1g} (P) \leftarrow ⁴T_{1g}) transition within the Co(II) ion (Mohamed et al., 2006; Kriza et al., 2011). This agrees with octahedral arrangement of ligands around the Co(II) ion. Similar structural arrangement has been reported for related Co(II) complexes of 1H-indole-2,3-dione derivatives (Kriza et al., 2011; A-Hassani et al., 2011). The new bands at 27041.64 cm⁻¹ and 27808.68 cm⁻¹ were due to ligand to metal charge transfer. Other d-d transitions were not observed probably due to their weak intensities caused by orbital relaxation and hence they were obscured by the more intense charge transfer bands. On the basis of the elemental analysis and electronic spectral data, an octahedral geometry may be proposed for this complex (Figure 1).

The electronic spectrum of 2 with the Lo spectrum showed that the free ligand's band centred at 22706.63 cm⁻¹ (440.40 nm) did not appear in the spectrum of 2. This may be due to very weak absorbance resulting from small

overlap between the ligand π orbitals and the metal e_g orbitals during complexation (Dunn et al., 1965). Evidence that the Ni(II) ion formed complex with the ligand is obvious from the bathochromic shift of the free ligand's absorption peak at 28296.55 cm^{-1} to 28200.80 cm^{-1} in 2 with increased intensity. The observed peak in 2 is probably due to ligand charge transfer. No $d-d$ transition was observed in 2 probably due to low intensity occasioned by orbital relaxation. Based on the result of Job's stoichiometric studies and elemental analysis, the complex, 2 tentatively proposed to be square planar.

Electronic spectrum of Lm is characterized by one broad absorption band of low intensity tailing the visible region with the peak at 24154.59 cm^{-1} . This band is attributed to $\pi^* \leftarrow \pi$ and $\pi^* \leftarrow n$ transitions within the ligand (Kriza et al., 2011). The spectrum also recorded four sharp peaks of close energies at the shoulder. These sharp peaks of strong intensities lie in the region 33670.03 – 38910.51 cm^{-1} . These bands are due to frequent intra ligand charge transfer (Dunn et al., 1965). These $\pi^* \leftarrow \pi$ and $\pi^* \leftarrow n$ transitions in the free ligand occurred in the metal complexes at lower wavenumbers than the ligands' indicating coordination of the ligand with the metals.

The electronic spectrum of 3 closely resembles that of Lm. It revealed two broad absorption bands and many sharp strong peaks and the shoulder centered between 34246.57 m^{-1} – 38535.65 cm^{-1} . These bands together with the absorption band at 23041.47 cm^{-1} are due to $\pi^* \leftarrow \pi$ and $\pi^* \leftarrow n$ transitions within the ligand moiety of the complex. These bands compared to those in the free ligand revealed both red and blue shifts indicative of complexation of the Lm with the Co(II) ion. Also observed is a new broad band at 20597.32 cm^{-1} due to $d-d$ transition within the Co(II) ion. In line with Job's

reaction ratio, molar conductance and electronic spectra of other Co(II) complexes reported (Raman et al., 2007) a square planar geometry was proposed. Consequently, the $d-d$ transition observed in this complex is assigned to ${}^1B_{1g} \leftarrow {}^1A_{1g}$ transition. The absorption bands due to ${}^4T_{2g}(\text{F}) \leftarrow {}^4T_{1g}$ and ${}^4A_{2g}(\text{F}) \leftarrow {}^4A_2$ transitions were not observed presumably due to weak intensity of the bands resulting from orbital relaxation (Lee, 1998). The electronic spectrum of 3 reaffirms the conviction that the Co(II) complexed with Lm despite the observed close resemblance of IR peaks of Lm and those of the 3.

Complex 4 gave one broad absorption band centred at 23310.02 cm^{-1} . This band belongs to $d-d$ transition within d orbitals of the Ni(II) ion. Complex 4 also recorded many sharp strong intensity bands characteristics of the ligand between 34246.58 cm^{-1} – 39215.69 cm^{-1} . These bands compared to those of Lm revealed both red and blue shifts which may be attributed to complexation. These high energy intense bands is due to spin allowed $\pi^* \leftarrow \pi$ and $\pi^* \leftarrow n$ transitions within the benzene rings in the ligand¹. Another new band in the spectrum of 4 at 23310.02 cm^{-1} is attributable to $d-d$ transition. Comparison with the electronic spectra of other Ni(II) complexes published in the literatures, (Dunn et al., 1965; Mohammed et al., 2006; Housecroft and Sharpe, 2008; Kriza et al., 2011) suggests an octahedral arrangement of the ligand around the Ni(II) ion and is assigned as ${}^3T_{1g}(\text{P}) \leftarrow {}^3A_{2g}$ transition. No ${}^3T_{2g} \leftarrow {}^3A_{2g}$ and ${}^3T_{1g}(\text{F}) \leftarrow {}^3A_{2g}$ were observed.

The spectrum of Lp revealed four broad weak absorption bands at 16350.56 cm^{-1} , 22644.93 cm^{-1} , 27442.37 cm^{-1} and 27855.15 cm^{-1} . These bands are likely due to $\pi^* \leftarrow \pi$ and $\pi^* \leftarrow n$ transitions in the ligand molecule. These transitions were also observed in the spectra of the metal complexes but they were shifted towards lower or higher frequencies

confirming the coordination of the ligand to the metal ions (Kriza et al., 2011).

The electronic spectrum of 5 gave bands at 15938.79 cm^{-1} , 16097.88 cm^{-1} , 24213.08 cm^{-1} , 27427.32 cm^{-1} and 27917.36 cm^{-1} were due to $\pi^* \leftarrow \pi$ and $\pi^* \leftarrow n$ transitions in the ligand fragment of the complex. The cobalt complex band at 27917.36 cm^{-1} compared to the free ligand's band at 27855.15 cm^{-1} revealed shift to higher wave number while the bands at 16097.88 cm^{-1} and 27427.32 cm^{-1} were shifted to lower wave numbers when compared to the free ligand's band at 16350.56 cm^{-1} and 2744.93 cm^{-1} respectively. These shifts from the absorption bands of the free ligand are evidence that the Co^{2+} complexed with the ligand and the shift probably was due to some dislocation of the π electrons in the ligand. New bands at 15938.79 cm^{-1} and 24213.08 cm^{-1} in the spectrum of this complex may be attributed to $d-d$ transitions in the $\text{Co}(\text{II})$ ion while the band at 28200.79 cm^{-1} was due to Co^{2+} to ligand charge transfer. The $d-d$ transitions are assigned as ${}^4\text{A}_{2g} \leftarrow {}^4\text{T}_{1g}(\text{F})$ (15938.79 cm^{-1}) and ${}^4\text{T}_{1g}(\text{P}) \leftarrow {}^4\text{T}_{1g}(\text{F})$ (24213.08 cm^{-1}) suggesting that there was an octahedral geometry of the ligand around the $\text{Co}(\text{II})$ ions (Dunn et al., 1965; Mohamed et al., 2006; Kriza et al., 2011). This also agrees with the geometry assigned to this complex in a similar synthesis reported in literature (A-Hassani, et al., 2011). The band representing the lower energy transition ${}^4\text{T}_{2g}(\text{F}) \leftarrow {}^4\text{T}_{1g}(\text{F})$ was not observed in this complex probably due to weak absorbance resulting from orbital relaxation (Dunn, 1965). The absence of ${}^4\text{T}_{2g}(\text{F}) \leftarrow {}^4\text{T}_{1g}(\text{F})$ transition was also reported⁴² though it was observed to be present in many $\text{Co}(\text{II})$ complexes of Schiff bases derived from 1H-indole-2,3-dione reported in the literature (Akpanisi, 2004).

The absorption bands of 6 appeared in the visible region. The free ligand's weak $\pi^* \leftarrow \pi$ and $\pi^* \leftarrow n$

absorption bands at 27442.37 cm^{-1} and 27855.15 cm^{-1} were not recorded for the $\text{Ni}(\text{II})$ complex. Also, the charge transfer absorption bands of the free ligand at 22644.93 cm^{-1} and 16350.56 cm^{-1} were shifted to 22935.78 cm^{-1} and 16097.88 cm^{-1} respectively in the nickel(II) complex. This red and bathochromic shifts in energy from the free ligand's bands 6 are indicative of complexation between $\text{Ni}(\text{II})$ ion and the ligand (Agbo and Ukoha, 2010; Ukoha et al., 2011). Three new absorption bands appeared in the spectrum of 6 at 13149.24 cm^{-1} , 13486.18 cm^{-1} and 15243.90 cm^{-1} . These were due to $d-d$ transitions within the $\text{Ni}(\text{II})$ orbitals. Based on the result of Job's stoichiometric measurement of this complex and the electronic spectra of other $\text{Ni}(\text{II})$ complexes (Dunn, 1965; Lee, 1998; Kriza et al., 2011). These transitions were assigned as ${}^3\text{T}_{2g} \leftarrow {}^3\text{A}_{2g}$ (13149.24 cm^{-1} -13486.18 cm^{-1}) and ${}^3\text{T}_{1g}(\text{F}) \leftarrow {}^3\text{A}_{2g}$ (15243.90 cm^{-1}) transitions indicative of octahedral geometry of 6 (Dunn, 1965; Lee, 1998; Kriza et al., 2011) (Figure 1).

Oral bioavailability of the 1H-indole-2,3-diones

Most drugs are administered orally for two major reasons: its convenience to patients and ease of manufacturing oral drugs. Therapeutic agents administered orally have to be adequately available in systemic circulation (orally bioavailable) in order to reach their target receptor/proteins (Mishra et al., 2012; Aungst, 2017). Lipinski proposed a rule, known as 'rule of five' (ro5) used to assess drug-likeness of potential drug molecules. The rule considers a drug candidate to be drug-like if it has; molecular weight (MW) < 500 Da, lipophilicity ($\log P$) < 5, hydrogen bond acceptor/donor (HBA/HBD) < 10/5 and number of rotatable bond (NRB) < 5 (Ibezim et al., 2015). The assessment is done in early drug development process so as to avoid waste of time and resource on compounds which will pose

physicochemical challenge. More stringent criteria were proposed to qualify compounds as both drug-like and drug leads termed lead-like criteria. It demands compounds to have $150 \leq MW \leq 350$, $\log P \leq 4$, $HBD \leq 3$, $HBA \leq 6$ and $NRB < 3$ (Ntie-Kang et al., 2014).

As shown in Table 4, all the compounds respected Lipinski's $ro5$. This indicates that the ligands will have

no problem permeating cell membrane to get adequate systemic exposure. Again, the compounds passed all the criteria for lead-likeness except for Lm and Lp which have slightly high MW. The physical properties of these three ligands suggest they are good drug-like and lead-like candidate. Therefore, we moved on to evaluate their ability to interact with drug targets.

Table 4. Main physic-chemical features of the ligand.

Title	MW(Da)	HBA	HBD	Log P	NRB
Lm	366.38	6	2	2.429	2
Lo	237.262	4	2	1.475	1
Lp	366.38	6	2	2.392	2

Docking calculations of the 1H-indole-2,3-diones

Based on literature reports that Schiff bases demonstrate antimicrobial properties, the ability of the ligands to interact with two validated antibiotic drug targets; penicillin binding protein (PBP) and DNA gyrase was investigated. The two proteins were used in this study because they are vital to the survival of the bacterial cell. PBPs play a major role in maintaining the integrity of bacterial cell wall while DNA gyrase relieves strains as double-stranded DNA is being unwound by helicases (Onoabedge et al., 2016, Nwuche et al., 2017). Moreover, both enzymes are absent in mammals. Table 5 showed that the docking protocols adopted in this study passed

the rmsd method of docking protocol validation requirement. The method accepts only dock protocol whose dock parameters produced a docked ligand whose pose deviates from that of x-ray crystallized ligand by $\leq 2 \text{ \AA}$.

Docking calculations on Lm, Lo and Lp revealed they demonstrated affinity for PBP and DNA gyrase (at ranges of -2.51 to -4.52 Kcal and -5.15 to -5.48 Kcal/mol respectively) (Table 6). This suggests the ligands might have antibiotic potency. In addition, the attractive physical-chemical properties of these ligands (Table 7) present them as promising starting materials for the development of a lead compound for the treatment of bacterial infections.

Table 5. Validation of docking protocol for native ligands toward the receptor site of the drug target.

Targets	Grid Points			Centre of Grid Box			ΔG (kcal/mol)	RMSD (\AA)
	X	Y	Z	X	Y	Z		
PBP	22	24	24	20.472	-11.823	40.666	-6.35	1.39
DNA gyrase	28	48	56	17.395	31.898	35.358	-4.49	2.09

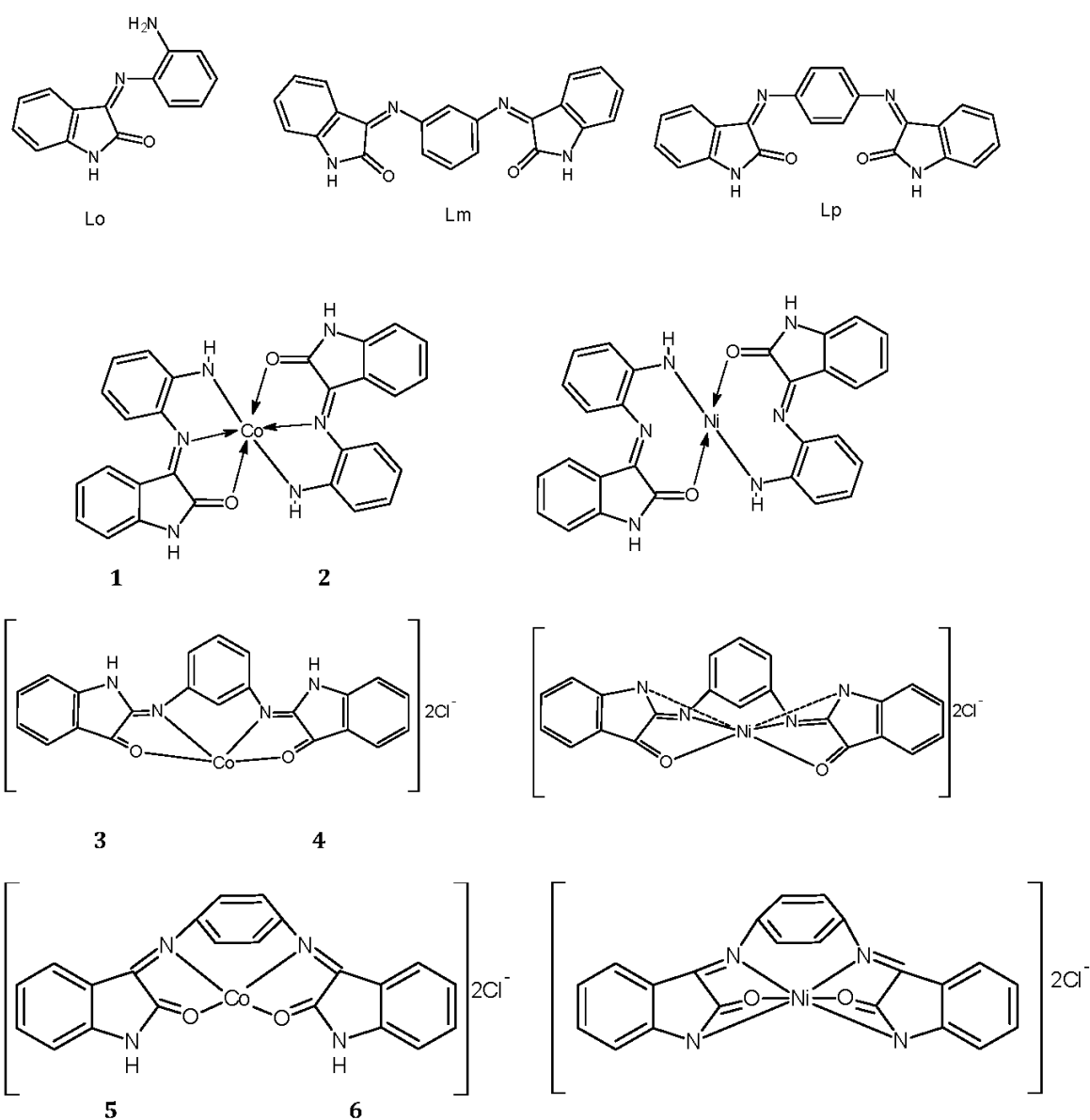


Figure 1. Structures of the ligands and complexes.

Table 6. Binding free energy of the ligands toward PBP and DNA gyrase.

Compounds	Lm	Lo	Lp
ΔG_{PBP} (kcal/mol)	-4.52	-3.36	-2.51
ΔG_{gyrase} (kcal/mol)	-5.15	-5.23	-5.48

Table 7. Theoretical free energy of binding of the complexes toward PBP and DNA gyrase.

Compounds	1	2	3	4	5	6
ΔG_{PBP} (kcal/mol)	-9.30	-9.20	-10.20	-9.40	-8.70	-10.20
ΔG_{gyrase} (kcal/mol)	-9.10	-9.20	-9.30	-7.30	-9.10	-9.50

It is widely reported that metal complexes of organic compounds tend to demonstrate improved therapeutic actions (Hassan, 1991; Raman et al., 2007; Singh et al., 2010). Therefore, Cobalt and Nickel complexes of the three compounds were prepared and docked toward PBP and DNA gyrase. Table 7 showed that the best docked conformation of all the metal-ligand complexes identified them as having improved interaction with the target proteins over the Schiff bases. This suggests that coordination of the organic compounds with Cobalt and Nickel metals activated the therapeutic action of the ligands and enabled better formation of target-ligand complex.

Antimicrobial tests results

The results of the *in vitro* antimicrobial screening of the ligands

and their complexes are presented in Table 8. The ligands Lo, Lm and Lp did not show any activity against the test microorganisms. However, upon chelation with Ni(II) and Ni(II) ions, the activity of the ligands increased significantly against most of the organisms. The Co(II) complex 1 showed low activity against *E. coli* 14 (2 mm) and *B. subtilis* (5 mm) but indicated zero activity against *P. aeruginosa* and *E. coli* 6. Its potency against *S. sciuri* was negligible (1 mm). [Ni(Lo)₂], 2 displayed moderate activity (7 mm) against *E. coli* 14 but had low activities against *E. coli* 6 and *S. sciuri* (4 mm, respectively). The MIC of 1 and 2 was 20 µg/mL. At lower concentrations, they showed no antibacterial potency.

Table 8. Antimicrobial activities of the ligands (Lo, Lm, Lp) and their complexes at 20 µg/mL.

Compound	Inhibition Zone of Diameter (mm)				
	<i>E. coli</i> (14) ATCC 25922	<i>E. coli</i> (6) ATCC 11105	<i>B. subtilis</i> (Isolated)	<i>S. sciuri subsp sciuri</i> ATCC 29062	<i>P. aeruginosa</i> ATCC 27853
Lo	-	-	-	-	-
Lm	-	-	-	-	-
Lp	-	-	-	-	-
1	2	-	5	1	-
2	7	4	-	4	-
3	28	30	24	20	26
4	-	6	2.3	7	2
5	7	8	4	9	-
6	29	35	29	45	30
Gentamicin	-	-	-	30	-
Ampicillin	-	-	34	40	32
Ciprofloxacin	34	30	-	-	-

“-“ indicates zero activity.

Complexes of Lm, 3 and 4 had enhanced antimicrobial activities. The Co(II) complex, 3 was most active against all the test bacteria compared to the other complexes. In fact, the IZD fell within 20 to 30 mm range with *E. coli* 6 showing the most sensitivity (30 mm)

and *S. sciuri* the least (20 mm). The MIC (Table 9) for *E. coli* 14 was 5 µg/mL (12 mm) while for the other strains, it was 10 µg/mL for *E. coli* 6 (16 mm), 5 µg/mL for *B. subtilis* (12 mm), 2.5 µg/mL for *S. sciuri* (13 mm) and 10 µg/mL for *P. aeruginosa* (15 mm). Complex 3 was

therefore the most active against *S. sciuri*. Its potency against *P. aeruginosa* and *S. sciuri* are comparable to those of the standard antibiotics [gentamicin (15 mm) and ampicillin (15 mm)] used as control. However, at 1.25 µg/mL concentration, the complex was not very active against *B. subtilis* which showed an IZD of 24 mm against standard antibiotic ampicillin. Results also show that the activity of complex against *E. coli* 14 and *E. coli* 6 strains were significantly lower

than that of the standard antibiotic ciprofloxacin. The nickel complex, [NiLm]Cl₂, 4 showed moderate activity against *E. coli* 6 (6 mm) and *S. sciuri* (7 mm) at 20 µg/mL (Table 9) concentration. It showed low activity against *B. subtilis* (2 mm) and *P. aeruginosa* (2 mm) and zero activity against *E. coli* 14. Below the 20 µg/mL concentration, 4 indicated no further activity against the test microorganisms.

Table 9. Minimum Inhibitory concentration (MIC) of the selected bioactive complexes measured in millimeter (mm) by the inhibition Zone Diameter (IZD)

Microorganism	Conc. of Compd. (µg/mL)	3	6	Gentamicin	Ampicillin	Ciprofloxacin
<i>E. coli</i> 14 ATCC 25922	10	15	15			
	5	12	13			
	2.5	-	-			
	1.25	-	-			17
<i>E. coli</i> 6 ATCC 11105	10	16	16			
	5	-	12			
	2.5	-	-			
	1.25	-	-			20
<i>B. subtilis</i> (Isolated)	10	15	15			
	5	12	13			
	2.5	-	10			
	1.25	-	-		24	
<i>S. sciuri</i> subsp <i>sciuri</i> ATCC 29062	10	20	20			
	5	17	15			
	2.5	13	14		15	
	1.25	-	12			
<i>P. aeruginosa</i> ATCC 27853	10	15	15			
	5	-	-			
	2.5	-	-	15		
	1.25	-	-			

1,4-phenylenediazanylylidenedi (1,3-dihydro-2H-indol-2-one) Lp was not

biologically active against the test microorganisms (Table 9). This contrasts

earlier investigation (A-Hassani et al., 2011) which reported significant activity against *B. subtilis*. However, the complex, [CoLpCl₂], 5 was active against *E. coli* 14 (7 mm), *E. coli* 6 (8 mm) and *S. sciuri* (9 mm) but only mildly active against *B. subtilis* (4 mm). It showed no effect against *P. aeruginosa*. The Ni(II) complex 6 displayed enhanced biological activities against the test microorganisms. At 20 µg/mL, the recorded activity was higher than data obtained from the three reference antibiotics; ciprofloxacin, ampicillin and gentamicin. The MIC (5 µg/mL) was same for *E. coli* strain 14 (13 mm) and strain 6 (12 mm), but was lower (2.5 µg/mL) for *B. subtilis* (10 mm). The MIC for *S. sciuri* (12 mm) was 1.25 µg/mL while that of *P. aeruginosa* (15 mm) was 10 µg/mL. [NiLp]Cl₂, 6 was the most potent against *S. sciuri* judging from the MIC value of 1.25 µg/mL which was lower than the concentration of 2.5 µg/mL obtained against the standard antibiotic (ampicillin). A detailed look at the biological activities of 3 and 6 show that while both complexes have high antibacterial potency, 6 had higher activity (as measured by the IZD) at lower MIC than 3. Thus, of all the complexes studied, 6 demonstrated an unmatched antibacterial potency as indicated by its 1.25 µg/mL MIC against *S. sciuri* and 2.5 µg/mL against *B. subtilis*. The activities of the complexes compared to those of the standard antibiotics (ciprofloxacin and ampicillin) revealed that the antibiotics were more potent against all the test organisms except *S. sciuri*; the organism to which complex 6 also indicated the highest activity against. In suitable solvents, 3 and 6 could be exploited as potential disinfectant and chemotherapeutic agents provided results from detailed pharmacologic and toxicological evaluations concerning human and animal safety are satisfactory.

The potency of the complexes against the test microorganisms unlike the free ligands is explainable by the chelation theory (Hassan, 1991; Raman

et al., 2007). In principle, the polarity of each metal ion on coordination with the ligands reduces due to its overlap with the ligand orbital and partial sharing of the positive charge of the metal ion with the donor groups within the chelate ring system (Hassan, 1991; Raman et al., 2007; Singh et al., 2010). Moreover, chelation increases the delocalization of π electrons over the whole chelate rings (Ibezim et al., 2015) leading to increase in the lipophilic nature of the central metal atom which in turn favours the permeation of the complexes through the lipid membranes while blocking the metal binding sites of the microbial enzymes and increasing the activity of the complexes (Singh et al., 2010; Mishra et al., 2012). These complexes interfere with microbial cellular respiration and block the synthesis of proteins which further inhibit the growth of the microorganisms (Raman et al., 2007). Other factors which could account for the observed increased antimicrobial activities of the complexes include solubility, dipole moment and conductivity of the metal complexes (Singh et al., 2012). In the present study, it was observed that the most potent complexes were those with high electrolytic conductance while the least ones were those with very low electrolytic conductance. This observation is in line with published ((Singh et al., 2012) reports which indicate that conductivity of metal complexes play significant roles in their antimicrobial activity.

The observed variations in the biological activities of the synthesized metal complexes have been explained with respect to liposolubility of the complexes. It has been reported that the lipid membrane surrounding the cell of microorganisms enables the passage of lipophilic compounds thereby making liposolubility an important factor affecting antimicrobial activity (Raman et al., 2007). The antimicrobial activities of the complexes therefore vary due to

differences in their permeability of the cell which in turn depends on their lipophilicity. The low activity of some of the metal complexes therefore may be due to their low lipophilicity which decreases their penetration through the lipid membrane of the test microorganisms and hence could neither block nor inhibit the growth of the microorganisms. The results of this study show that the farther apart the two amino groups of the benzenediamine moiety of the complexes are from each other, the more potent the complex against the microorganisms. Whereas the complexes resulting from benzene-1,2-diamine showed low biological activity against all the microorganisms screened *in vitro*, the complexes from benzene-1,3-diamine showed better biological activity under the same conditions. However, the complexes derived from benzene-1,4-diamine showed the greatest activity against the test microorganisms. One can conclude tentatively, that the degree of lipophilicity of the prepared complexes may depend on the relative position of the amino/ azomethine groups of the complexes.

Analysis of binding mode of 3 and 6

The complexes, 3 and 6, demonstrated greater affinity for both PBP and DNA gyrase over the rest and further proved their therapeutic supremacy by killing the test bacteria at lower MIC than the approved drugs. The unique binding poses of 3 and 6 toward PBP (Figure 2a and 2b) within the lipophilic cavity suggest both complexes adopted configuration which enabled their phenyl groups to interact better with TYR306, THR116 and TRP233 aromatic rings and to make hydrogen bonding with ASN161 carboxylate moiety. In a similar way, conformations of the complexes were also identified to play a major role in accommodating them within the lipophilic pocket of DNA gyrase binding site (Figure 1c and 1d). Observation showed that interactions were, in general, characterized by hydrophobic bonding. In addition, the structure of the complexes appeared to be responsible for accommodating them properly within the target active sites and penetration into bacteria to inactivate essential enzymes and finally kill it.

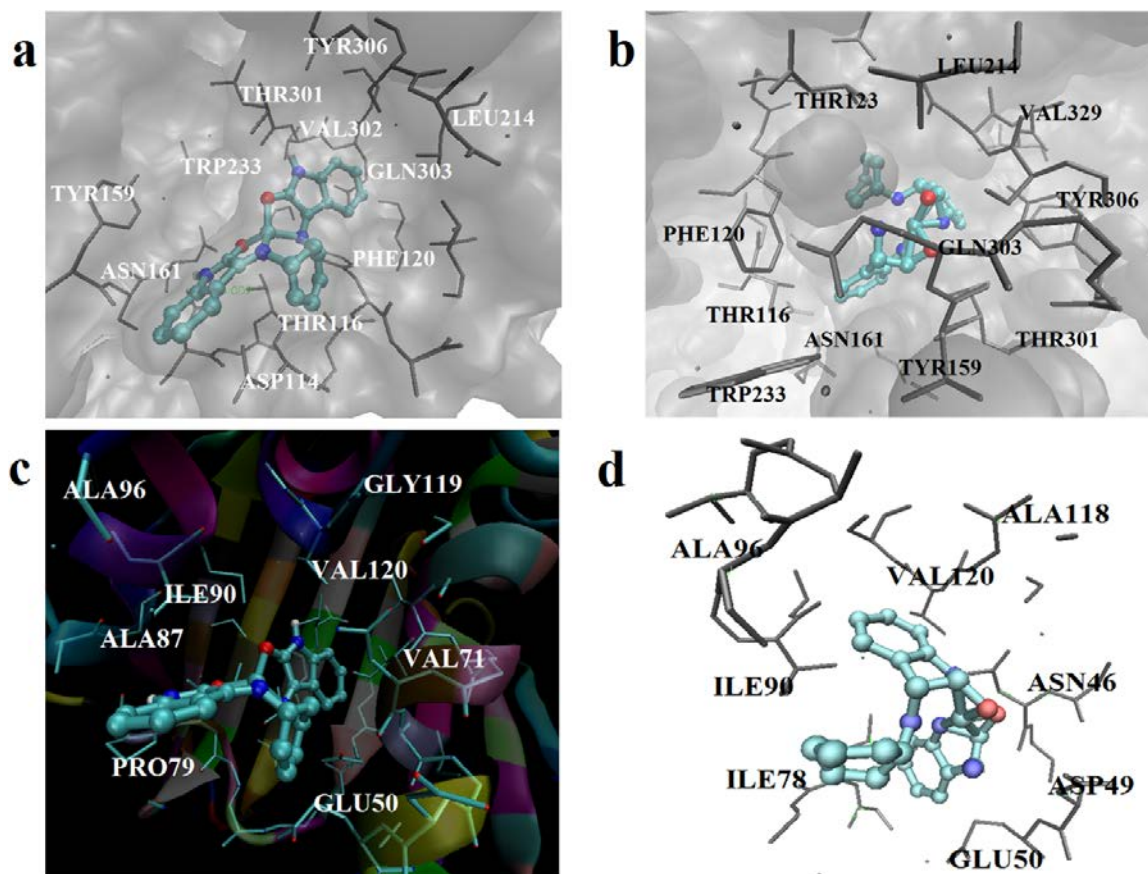


Figure 2. Binding orientations of **3** and **6** overlaid in the active sites of PBP (a and b, respectively) and DNA gyrase (c and d, respectively).

Conclusion

Rising cases of antibiotic drug resistance has kept all hands on deck in search of ways to improve current antibiotics and/or discover/design new antibacterial agents. Effort was made in the current work to develop antibacterial drug lead(s) from 1*H*-Indole-2,3-dione scaffold and their cobalt and nickel complexes. Docking studies of the organic compounds and their complexes suggested that the interactions of the ligands with the chosen antibacterial drug targets (PBP and DNA gyrase) were improved by the presence of the metal ion (their metal complexes). Experimental screening of the compounds against five selected bacteria strains confirms their antibiotic potencies and further showed that

coordination of ligand with metal ion enhanced/activated their therapeutic action. Two complexes, **3** and **6**, killed the test bacteria at MIC lower than the used approved antibiotic drugs. Therefore, their binding modes were studied and the identified interactions could be targeted in structure optimization process.

Conflicts of interest

The authors declare no conflict of interest relevant to this article.

References

A-Hasani, R. A. M.; Mohammed, S. M.; Rasheed, E. M. Synthesis, characterization and biological study of Cr(III), Mn(II), Co(II), Ni(II), Cu(II) and Zn(II) complexes with a new tetradentate Schiff base ligand. **Iraqi**

National Journal of Chemistry, v. 43, p. 392-398, 2011.

Abdul-Manam, M. A. F.; Cordes, D. B.; Slawin, A. M. Z.; Buhl, M.; Liao, V. W. Y.; Chua, H. C.; Chebib, M.; O'Hagen, D. The synthesis and evaluation of fluoro-, trifluoromethyl and iodomuscimols as GABA agonists. **Chemistry**, v. 23, p. 10848-10852, 2017.

Agbo, J. N.; Ukoha, P. O. Synthesis, characterization and preliminary antimicrobial activities of some azo ligands derived from aminoantipyrine and their Co(II), Fe(III), and Os (VIII) complexes. **International Journal Chemistry**, v. 20, p. 217-225, 2010.

Akpanisi, L. E. S. **Organic spectroscopy**. Nigeria: Loius Chumez Printing Enterprises, 2004.

Aungst, B. J. Optimizing oral bioavailability in drug discovery: An overview of design and testing strategies and formulation options. **Journal of Pharmaceutical Sciences**, v. 106, p. 921-929, 2017.

Berman, H. M.; Westbrook, J.; Feng, Z.; Gilliland, G.; Bhat, T. N.; Weissig, H. Shindyalov, I. N.; Bourne, P. E. The protein data bank. **Nucleic Acids Research**, v. 28, p. 235-342, 2000.

Bhrigu, B.; Pathak, D.; Siddiqui, N.; Alam, S. M.; Ahsam, W. Biological activity of indoline derivatives. **International Journal of Pharmacy Sciences and Drug Research**, v. 2, p. 229-234, 2010.

Bollenbach, T. Antimicrobial interaction: Mechanisms and implications for drug discovery and resistance evolution. **Current Opinion in Microbiology**, v. 27, p. 1-9, 2015.

Breitmaier, E.; Voelter, W. **Carbon-13 NMR spectroscopy**. 3. ed. Weinheim: VCH, 1987.

Cerchiaro, G.; Ferreira, A. M. D. Oxindoles and copper complexes with oxindole: Derivatives as potential pharmacological agents. **Journal of the Brazilian Chemical Society**, v. 17, p. 1473-1485, 2006.

CCG - Chemical Computing Group. Molecular Operating Environment (MOE). Software Edition, 2010.

Chinnasamy, R. P.; Sundararajan, R.; Govindaraja, S. Synthesis, characterization and analgesic activity of novel Schiff base of isatin derivatives. **Journal of Advanced**

Pharmaceutical Technology & Research, v. 1, p. 342-347, 2010.

Dunn, M. T.; McClure, D. S.; Pearson, B. C. **Some aspects of Crystal Field Theory**. New York: Harper and Row Publishers, 1965.

Halgren, T. A. Merck molecular force field. **Journal of Computational Chemistry**, v. 17, p. 490-641, 1996.

Hassan, A. M. Co(II) and Fe(II) Schiff base chelates derived from isatin and some amino acids. **Medical Journal of Islamic World Academy of Sciences**, v. 4, p. 271-294, 1991.

Housecroft, C. E.; Sharpe, A. G. **Inorganic Chemistry**. 3. ed. London: Pearson Education England, 2008.

Ibezim, A.; Nwodo, N. J.; Nnaji, N. J. N.; Ujam, O. T., Olubiyi, O. O.; Mba, C. J. In-silico investigation of morpholines as novel class of trypanosomal triosephosphate isomerase inhibitors. **Medicinal Chemistry Research**, v. 26, p.180-189, 2016.

Ibezim, A.; Debnath, B.; Ntie-Kang, F.; Mbah, C. J.; Nwodo, N. J. Binding of anti-trypanosome natural products from African flora against selected drug targets: A docking study. **Medicinal Chemistry Research**, v. 26, p. 562-579, 2017.

Ibezim, A.; Olujide, O. O.; Ata, K.; Mbah, C. J.; Nwodo, N. J. Structure based study of natural products with anti-schistosoma activity. **Current Computer-Aided Drug Design**, v. 13, p. 91-100, 2017.

Ibezim, A.; Onyia, K.; Ntie-Kang, F.; Nwodo, J. N. Drug like properties of potential anti-cancer compounds from Cameroonian flora: A virtual studies. **Journal of Applied Pharmaceutical Science**, v. 5, p. 133-137, 2015.

Iman, S. A.; Varma, R. S. Isatin-3-anils as excystment and cysticidal agents against *Schizopyrenes russelli*. **Experimentia**, v. 31, p. 1287-1288, 1975.

Kazuma, N.; Shigeru, K.; Fujio, T.; Masaki, H.; Yoshio, I. Condensation of isatin with O-phenylenediamine. **Bulletin of the Chemical Society of Japan**, v. 55, p. 2293-2294, 1982.

Kriza, A.; Ignat, I.; Stanica, N.; Draghici, C. Synthesis and characterization of Cu(II), Co(II) and Ni(II) complexes with Schiff bases derived from isatin. **Revista de Chimie**, v. 62, p. 696-701, 2011.

- Lee, J.D. **Concise Inorganic Chemistry**. 5. ed. New York: Black Well Science, 1998.
- Manan, M. F.; Karimah, K.; Abdul-Manan, M. A. F. Synthesis, characterization and conductivity studies of Schiff base ligand derived from isatin and o-phenylenediamine with its Cobalt(II) metal complex and Lithium-Schiff base compound. **The Malaysian Journal of Analytical Sciences**, v. 16, p. 318-324, 2012.
- Mashaly, M.M.; Abd- Elwahab, Z.H.; Faheim, A. Preparation, special characterization and antimicrobial activities of Schiff base complexes derived from 4-aminoantipyridine mixed ligand complexes with 2-Aminopyridine, 8-hydroxyquinoline and oxalic acid and their pyrolytical products. **Journal of the Chinese Chemical Society**, v. 51, p. 901-915, 2004.
- Medvedev, A. E.; Clow, A.; Sandler, M.; Glover, V. Isatin: A link between natriuretic peptides and monoamines? **Biochemical Pharmacology**, v. 52, p. 385-391, 1996.
- Mishra, A. P.; Mishra, R.; Jain, R.; Gupta, S. Synthesis of new Vo(II), Co(II), Ni(II) and Cu(II) complexes with isatin-3-Chloro-4-floroaniline and 2-pyridinecarboxylidene-4-aminoantipyrine and their antimicrobial studies. **Mycobiology**, v. 40, p.20-26, 2012.
- Mohamed, G. G.; Omar, M. M.; Hindy, A. M. Metal complexes of Schiff bases: Preparation, characterization and biological activity. **Turkish Journal of Chemistry**, v. 30 p. 361-382, 2006.
- Morris, G. M.; Goodsell, D. S.; Halliday, R. S.; Huey, R.; Hart, W. E.; Belew, R. K.; Olson, A. J. Automated docking using a larmarekian genetic algorithm and emperical binding free energy function. **Journal of Computational Chemistry**, v. 19, p. 1639-1662, 1998.
- Nagajothi A.; Kiruthika A.; Chitra S.; Parameswari, K. Synthesis and characterization of Tetradentate Co(II) Schiff base complexes: Antimicrobial and DNA cleavage studies. **International Journal of Pharmacy and Biomedical Sciences**, v. 3, p. 1768-1778, 2012.
- NCCLS - National Committee for Clinical Laboratory Standards. **Methods for dilution antimicrobial susceptibility tests for bacteria that grow aerobically**: Approved standard m7-A3. 3. ed. Villanova, PA: NCCLS, 1993.
- Ntie-Kang, F.; Nwodo, J. N.; Ibezim, A.; Simoben, C.V.; Karaman, B.; Ngwa, V.; Sippl, W.; Adikwu, M.U.; Mbaze, L. M. Molecular modeling of potential anticancer agents from African medicinal plants. **Journal of Chemical Information and Modeling**, v. 54, p. 2433-2450, 2014.
- Nwuche, C. O.; Ujam, O. T.; Ibezim, A.; Ujam, I. B. Experimental and in-silico investigation of anti-microbial activity of 1-chloro-2-isocyanatoethane derivatives of thiomorpholine, piperazine and morpholine. **PLoS ONE**, v.12, e0170150, 2017.
- Onoabedje, E. A.; Ibezim, A.; Okafor, S. N.; Onoabedje, U. S.; Okoro, U. C. Oxazin-5-ones as a novel class of penicillin binding protein inhibitors: design, synthesis and structure activity relationship. **PLoS ONE**, v. 11, e0163467, 2016.
- Pandeya, S. N.; Sriram, D. Synthesis and antimicrobial activity of Schiff's and Mannich bases of isatin and its derivatives. **Acta Pharmaceutica Turcica**, v. 40, p. 33-38, 1998.
- Pandeya, S. N.; Sriram, D.; Nath, G.; Clercq, E. Synthesis, antibacterial, antifungal and anti-HIV evaluation of Schiff and Mannich bases of isatin and its derivatives with triazole. **Arzeimittelforschung**, v. 50, p. 55-59, 2000.
- Pandeya, S. N.; Sriran, D.; Nath, G.; De Clercq, E. Synthesis, antibacterial, antifungal and anti-HIV activities of norfloxacin Mannich bases. **European Journal of Medicinal Chemistry**, v. 35, p. 249-255, 2000.
- Pandeya, S. N.; Yogeewari, P.; Sriram, D.; De Clercq, E.; Pannecouque, C.; Witvrouw, M. Synthesis and screening for anti-HIV activity of some n-Mannich bases of isatin derivatives. **Chemotherapy**, v. 45, p. 192-196, 1999.
- Raman, N.; Raja, J.; Sakthivel, A. Synthesis, spectral characterization of Schiff base transition metal complexes: DNA cleavage and antimicrobial activity studies. **Journal of Chemical Sciences**, v. 119, p. 303-310, 2007.
- Reddy, R. K.; Suneetha, K.; Karigar, C. S.; Manjunth, N.; Mahendra, K. Cobalt(II), Ni(II), Cu(II), Zn(II), Cd(II), Hg(II), UO₂(VI) and th(IV) complexes from ONNN Schiff base ligand. **Journal of the Chilean Chemical Society**, v. 53, p. 1653-1657, 2008.

- Sarangapani, M.; Reddy V. M. Pharmacological screening of isatin-[N-(2-alkyl benzoxazole-5-carbonyl)]hydrazones. **Indian Journal of Pharmaceutical Sciences**, v. 59, p. 101-105, 1977.
- Silva, J. F. M.; Garden, S. J.; Pinto, A. C. The chemistry of isatins: A review from 1975 to 1999. **Journal of the Brazilian Chemical Society**, v. 12, p. 273-324, 2001.
- Singh, A. K. Inhibition of mild steel corrosion in hydrochloric acid solution by 3-(4-((Z)-indolin-3-ylideneamino) phenylimino) indolin-2-one. **Industrial & Engineering Chemistry Research**, v. 51 p. 3215-3223, 2012.
- Singh, D. P.; Grover, V.; Kumar, K.; Jain, K. Metal ion prompted macrocyclic complexes derived from Indole-2,3-dione (isatin) and O-phenylenediamine with their spectroscopic and antibacterial studies. **Acta Chimica Slovenica**, v. 57, p. 775-780, 2010.
- Singh, P.; Dandia, A.; Khandelwal, A. Facile chemoselective synthesis of novel 6-aryl-12H-indole [2, 3-e]{1,4}benzodiazocine derivatives by reaction of 3-arylmethylene-2H-indol-2-ones with o-phenylenediamine. **Indian Journal of Chemistry**, v. 49, p. 1135-1139, 2010.
- Tagg, J. R.; Mc-Given, A. R. Assay system for bacteriocins. **Applied Microbiology**, v. 21, p. 943, 1971.
- Todeschini, A. R.; De Miranda, A. L. P.; Da Silva, K. C. M.; Parrini, S. C.; Barreiro, E. J. Synthesis and evaluation of analgesic, anti-inflammatory and antiplatelet properties of new 2-pyridylarylhydrazone derivatives. **European Journal of Medicinal Chemistry**, v. 33, p. 189-200, 1998.
- Ukoha, P. O.; Alioke, C. U.; Obasi, V. L.; Chah, K. F. Synthesis, spectroscopic characterization and preliminary antimicrobial studies of Mn(II) and Cu(II) complexes of two thiolates; S, S1-(2, 6-Diaminopyridine-3,5-Diyl-dibenzene Carbothioate (DBCT) and S-Benzyl Benzene Carbothioate (BBCT). **Journal of Chemistry**, v. 8, p. 231-239, 2011.
- Varma, R. S.; Nobles, W.L. Antiviral, antibacterial, and antifungal activities of isatin N-Mannich bases. **Journal of Pharmaceutical Sciences**, v. 64, p. 881-882, 1975.
- Verma, R. S.; Khan, I. A. Occurrence of extra-ovarian ovules in sunflower plants (*Helianthus annus* L.) treated with chloroflurenol. **Polish Journal of Pharmacology and Pharmacy**, v. 29, p. 549-594, 1977.
- Wu, H. L.; Gao, Y. C. Synthesis, crystal structure and characterization of zinc (II) complexes with the tripod ligand tris(2-benzimidazolylmethyl)amine and α,β -unsaturated carboxylates. **Transition Metal Chemistry**, v. 29, p. 175-179, 2004.



License information: This is an open-access article distributed under the terms of the Creative Commons Attribution License, which permits unrestricted use, distribution, and reproduction in any medium, provided the original work is properly cited.